

Integrated moulded polymer electrodes for performing conductivity detection on isotachopheresis microdevices

S.J. Baldock*, P.R. Fielden, N.J. Goddard, J.E. Prest, B.J. Treves Brown

Department of Instrumentation and Analytical Science (DIAS), UMIST, P.O. Box 88, Manchester M60 1QD, UK

Abstract

The feasibility of using integrated injection moulded polymer electrodes as drive and detection electrodes for performing miniaturised isotachopheresis (ITP) separations with conductivity detection has been demonstrated. Injection moulded electrodes were produced from three different grades of carbon-filled polymer. Two of the electrode designs were found to be suitable for performing on-chip conductivity detection. The high-voltage characteristics of the microdevices were found to be suitable for performing ITP, with a power dissipation up to 1.4 W m^{-1} being achieved. Three model separations are presented to demonstrate the separation capability of the miniaturised injection moulded devices. Three anionic dyes, two inorganic anions and a mixture of eight alkaline earth, transition and lanthanide metal cations were analysed.

© 2002 Elsevier Science B.V. All rights reserved.

Keywords: Conductivity detection; Detection, electrophoresis; Isotachopheresis; Instrumentation; Electrodes; Chip technology; Inorganic anions; Metal cations; Dyes

1. Introduction

Recent reviews by Becker and co-workers [1,2] on the subject of polymer microfluidic devices (sometimes known as laboratory-on-a-chip devices) intimate that the dominance of glass, as a substrate material for miniaturised separation devices, may be diminishing as increasing numbers of researchers and commercial manufacturers realise the advantages of using plastics in device construction. The benefits of employing plastics include: the low cost and wide range of raw materials available and the amenability of such materials to surface modification techniques. Many polymer processing methods are compatible with mass fabrication techniques, hence greater

reproducibility in device-to-device production can be achieved. Plastics also offer easier fabrication of channels with different wall geometries and heights compared to glass. Many methods are applicable for the formation of channel structures in polymer materials. The majority of devices reported have used hot embossing (with metal or silicon wafer stamps) to impress a channel pattern into a plastic plate. Injection moulding using nickel electroforms of silicon wafers as mould cavities has also been widely reported. Casting of elastomeric polymers against silicon wafers and metal moulds have mainly been reported by workers within the academic community, as the curing time of the resin is generally slow and hence is less ideally suited to mass production. Other direct fabrication methods such as laser photoablation using excimer lasers and layering methods employing photoresist materials, e.g. SU8, have also been used to create polymeric

*Corresponding author. Tel.: +44-161-200-8900; fax: +44-161-200-4896.

E-mail address: sara.baldock@umist.ac.uk (S.J. Baldock).

devices. Sealing of devices has been accomplished via a number of different methods such as lamination, gluing, thermal bonding and laser and ultrasonic welding [2]. To date sputtering, thermal deposition and electron beam evaporation have been used to deposit thin metal layers to form electrodes. These methods are normally constrained to planar devices as deposition is more complex on three-dimensional structured chips [2].

Injection moulding has been selected as the processing method of choice in this study, as in addition to providing reproducible planar channel assemblies quickly and at a reasonable cost, injection moulding allows the incorporation of structures in the third dimension. For example, sample and electrolyte reservoirs can be realised within the substrate half that defines the sample channels and preformed elements, such as electrodes, can be integrated into the moulded device.

The majority of published applications of microdevices have utilised electroseparation methods, most using capillary electrophoresis (CE) [2]. Notwithstanding this interest shown in miniaturised CE devices, the use of microdevices for isotachopheresis (ITP) separations has been reported by only a few groups in addition to ourselves.

An early approach to system integration for ITP was reported in 1975. Boček et al. [3] described a downscaled ITP instrument formed from a monolithic Perspex block which incorporated electrode compartments, stopcocks and a milled 1.0 mm×0.2 mm capillary. In 1983 a separation of nitrate, chloride and sulphate in drinking water employing similar technology was reported [4]. In addition to miniaturised ITP devices fabricated from glass [5,6], our earlier reported work on ITP microdevices include microchannels formed from cast moulded silicone elastomer bonded onto printed circuit boards to form electrode bearing devices. The polychlorinated biphenyl boards incorporated gold microband electrodes for conductivity detection and gold disc electrodes for application of the separation voltages. Using this device, separations of various dyes and a three-component transition metal sample were reported [7,8]. Silicone elastomer channels were also adhered to glass substrates with either thin film gold and platinum electrodes to form integrated devices [9], separations of a three-component metal ion

mixture and a sample consisting of three nucleotides were presented [10]. A cast moulded device formed from two sheets of a silicone elastomer with on-column single platinum electrode conductivity detection was first reported in 1999, with a separation of potassium and sodium ions [11]. This was later followed by a separation of four metal ions; lithium, lanthanum, dysprosium and ytterbium [12]. Devices fabricated using dryfilm photoresist to form channel structures with screen printed detection electrodes have also been demonstrated [10]. Latterly our research effort has focused on the production of injection moulded devices. Injection moulded devices with overmoulded metal drive electrodes and spherical lenses for optical detection were reported in 2000 [13], while moulded devices incorporating drive and detection electrodes formed from chemically milled gold plated copper sheets were presented in 2001 [10]. In 2002, our group presented the first report of the use of micromoulding to produce devices which incorporated polymer drive and detection electrodes, two integrated electrode devices were presented and a preliminary separation of amaranth demonstrated [14].

Other current progress in the miniaturisation of ITP separation devices has revolved around the development in 2001 of a hot embossed poly(methyl methacrylate) (PMMA) microchip with integrated sputtered thin film platinum electrodes by Grass et al. [15]. The device consisted of four channel compartments; two sample loops of differing volumes, a pre-separation and an analytical column and three planar buffer reservoirs all with a depth of 200 µm. This device has subsequently been used by Masár et al. for the ITP analysis of organic acids and inorganic anions in red and white wines [16]. ITP separations of a 14-component model mixture were reported [17], in addition to the separation of tryptophan enantiomers [18]. Chip-to-chip performance and repeatability studies on the separation of a three-component anion mixture were also presented [19] along with an investigation of the conductivity cell geometry of the detector electrodes [20]. The PMMA devices have also been used for ITP–capillary zone electrophoresis (CZE) separations. Kaniansky et al. reported the separation of a three-anion mixture [17] and Bodor et al. reported the determination of six inorganic anions in water sam-

ples [21] and the analysis of food and cosmetic additives [22]. Recently the separation of three selenoamino acids by ITP–CZE was reported by Grass et al. [20,23] and the determination of oxalate in urine using CZE was reported by Zúborová et al. [24]. Optical detection of the temperature differences between ITP zones using diode laser absorption spectroscopy was also attempted on the PMMA microdevice with limited success [25]. Optical detection has also been investigated by Walker et al. who used Raman spectroscopy to detect a partially resolved herbicide ITP separation on a glass device [26].

This paper presents the potential of using preformed moulded polymer electrodes as inserts in injection moulded devices to form drive and conductivity electrodes. Fabrication of the devices is described and electrodes formed from three different grades of conducting polymer are appraised with respect to their suitability for performing conductivity detection. The microdevices are moulded from two different polymeric materials and all devices presented have two diametrically opposed electrodes for detection. Performance of the devices under high voltage conditions and for carrying out ITP separations was evaluated.

2. Experimental

2.1. Chemicals and solutions

For the anionic dye separations, the leading electrolyte (LE) was 0.01 M HCl (0.1 M HPCE grade, Fluka, Gillingham, UK) adjusted to pH 6 with L-histidine (>99%, Sigma, Gillingham, UK). Hydroxyethylcellulose (HEC) 0.1% (w/v) (molecular mass ca. 250 000, Aldrich, Gillingham, UK) was added to suppress any electroosmotic flow. The terminating electrolyte (TE) was 0.01 M 2-(*N*-morpholino)ethanesulfonic acid (MES) (>99.5%, Sigma) adjusted to pH 6 with histidine. The anionic dye samples were prepared from 0.01 M stock solutions of amaranth (Aldrich), bromophenol blue (Acros, Loughborough, UK) and methyl orange (Aldrich). For the inorganic anion separations, the LE was 0.01 M HCl adjusted to pH 3.6 with glycylglycine (99+%, Acros) and 0.1% (w/v) HEC

was added. The TE was 0.01 M benzoic acid (AnalaR grade, BDH, Merck, Poole, UK). Inorganic anion samples were prepared from 1000 ppm fluoride standard solution (Aldrich) and sodium nitrite (99.99%, Aldrich). For the metal cation electrolyte system, the LE was 0.02 M NaOH (1 M volumetric standard, Aldrich) with 0.015 M 2-hydroxyisobutyric acid (HIBA) (98+%, Aldrich) added as a complexing agent and adjusted to pH 4.95 using propionic acid (99.6%, Sigma). HEC 0.05% (w/v) was added. The TE was 0.01 M DL-carnitine hydrochloride (98+%, Sigma). Stock solutions (0.05 M) of individual metals were prepared from the following chloride salts: calcium chloride dihydrate salt (99+%, Aldrich), manganese chloride tetrahydrate (98+%, Aldrich), magnesium chloride hexahydrate (99%, Aldrich), cobalt chloride hexahydrate (98%, Aldrich), nickel chloride hexahydrate (98%, BDH), zinc chloride (98+%, Aldrich), lanthanum chloride heptahydrate (99.9%, Aldrich), neodymium chloride hexahydrate (99.9%, Aldrich), gadolinium chloride hexahydrate (99.9%, Aldrich) and copper chloride dihydrate (Riedel-de-Haën, Gillingham, UK). The standard conductivity cell calibration solution (0.1 M) was prepared from dried KCl (AnalaR, BDH). All solutions were prepared using >18 M Ω water (Elga Maxima Ultra Pure, Vivendi, High Wycombe, UK).

2.2. Fabrication of injection moulded devices

The complete fabrication procedure for the manufacture of the injection moulded ITP systems, from mould design to device sealing was carried out in-house. Designs for injection moulded devices were created using AutoCAD Mechanical Desktop v5.0 (Autodesk, San Jose, CA, USA). The solid models produced using this package were converted to toolpaths using EdgeCAM v6.75 (Pathtrace, Reading, UK). EdgeCAM generates ISO G-Code CNC files that are converted into the macro commands required for the precision CNC milling machine. The milling machine, a Datron CAT3D M6 (Datron Technology, Milton Keynes, UK), uses conventional tungsten carbide end mills and drills. The moulds used in this work were created using a 1 mm drill with a 2° tapered draft angle to facilitate proper ejection of the moulded piece from the mould cavity.

A 0.3 mm diameter end mill was used to make the finishing cut. Milled brass moulds are normally used, as brass is a hard material with a good surface finish, however, aluminium, though a less hard wearing material, has also been utilised for some of our mould inserts without any noticeable detrimental effect on the moulding procedure. The milled moulds produced are accommodated on steel tool platens housing the ejector pins and injection gate in the moulding machine. For the first electrode design (see Fig. 1) the mould cavity had recesses and conduits on one half of the template (which form the relief mould for the electrodes), into which a conducting polymer could subsequently be injected to create the electrodes; the separation channel and access reservoirs were located on the other half of the mould. A complete device was formed by dicing the mould in half after the electrode formation stage. The two halves were then ready for bonding.

For the second and third electrode designs (where overmoulding of preformed components was performed), two sets of mould cavities were produced to fabricate the ITP devices. The first set was milled with the design to form the drive and detection electrodes, while the second set was patterned with the inverse relief of the channel network, along with pillars (which form solution reservoirs). Recesses and pins were also incorporated into this mould cavity, which hold the electrode elements in place during the second moulding process. Electrode design two (see Fig. 2) had planar electrodes, whilst electrode design

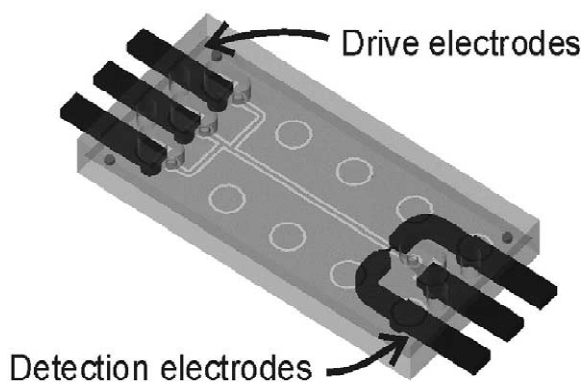


Fig. 1. A representation of a microdevice with electrode design 1. Devices were fabricated by injection moulding conducting polymer into a preformed polystyrene part. The device had a separation channel of length 19.9 mm.

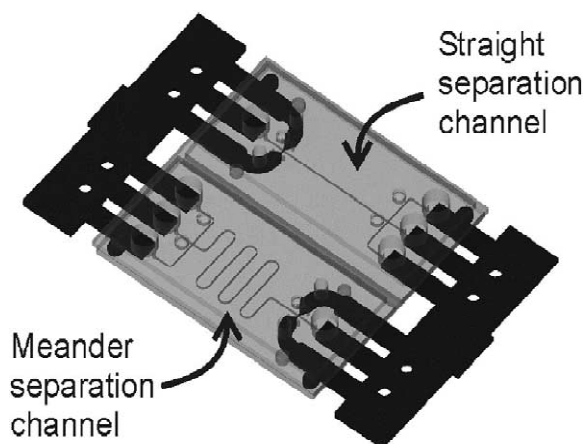


Fig. 2. A representation of a microdevice with electrode design 2, incorporating two distinct separation channels. Separation channels had lengths of 19.2 mm (straight) and 74.2 mm (meander). Fabrication of the device was by overmoulding of preformed conducting electrode assemblies.

three (see Fig. 3) had three dimensionally structured electrodes. The injection moulding machine used in this work to produce the electrodes was a Babyplast 6/6, whilst a Babyplast 6/10 (Cronoplast, Spain) was used to mould the microdevices. The Babyplasts are automatic injection moulding machines capable of moulding devices with a component weight of up to 7 g of plastic.

A large variety of plastic materials can be injection moulded. This group has moulded microdevices from the following materials: PMMA, polycarbonate (PC), crystal polystyrene (PS), high impact polystyrene (HIPS), Surlyn[®] ionomer (a sodium neutralised ethylene/methacrylic acid copolymer, DuPont), as well as two cyclo-olefin polymers (COPs); Zeonex (an amorphous norbornene homopolymer) and Zeonor (an amorphous norbornene–ethene copolymer) both from Nippon Zeon (Cardiff, UK). The chip materials used in this study were polystyrene (Northern Industrial Plastics, Chadderton, UK) and Zeonor 1060R (Nippon Zeon). These materials were selected on the basis of their advantageous physical properties (low mould shrinkage, high rigidity, and good optical clarity) as well as for their good chemical resistance.

A range of carbon-filled plastic materials are available, which have found applications, e.g. antistatic and electromagnetic interference (EMI) shield-

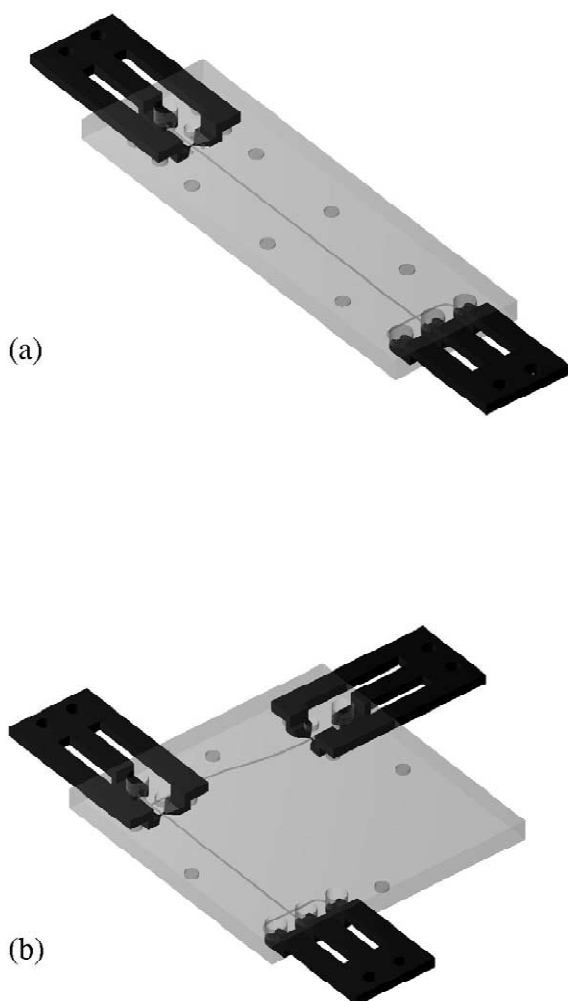


Fig. 3. A representation of microdevices with electrode design 3. A single column (1D) chip is shown in (a) with a channel length of 44 mm, while (b) depicts a two column (2D) device incorporating detection electrodes at the end of each channel, with a separation length of 54.4 mm to the final detection electrodes. Fabrication of the device was by overmoulding of preformed conducting electrode assemblies.

ing, where conductivity is important. Three types of filled plastic were evaluated in this study. The first was an 8% carbon black filled polystyrene (Northern Industrial Plastics). The second material was a 40% carbon fibre filled nylon 6/6 (grade: RC-1008, LNP Engineering Plastics, Solihull, UK). The third was a 40% carbon fibre filled HIPS (RTP 487, RTP Company UK Plastics, Bury, UK).

The final stage in the preparation of an integrated ITP device is to bond or seal the produced injection moulded parts to form a complete device. Sealing of the first electrode device design was accomplished by bonding the channel containing half to the substrate accommodating the electrodes with cyanoacrylate glue. Precise alignment was attained through the use of locating pegs and matching recesses incorporated into the mould design. Sealing of chips with electrode designs two and three was achieved using a self-adhesive polyester laminate (Plastic Art, Manchester, UK). The drive and detection electrodes were then electrically isolated by cutting away excess polymer to form a device ready for use.

Table 1 presents a summary of the devices fabricated. In total, four different devices were constructed with three different electrode designs. Three chip designs featured single dimensional (1D) separation columns. In addition to straight channel designs, a meander was incorporated onto one device. One design featured two columns forming a two-dimensional (2D) separation device that incorporated two sets of detection electrodes. Fig. 4 shows the cross-sectional profiles and plan views of the resulting electrode designs.

2.3. Instrumentation for performing ITP separations on microdevices

The instrumentation system comprises of a high-voltage (HV) programmable power supply unit (PSU), a fluid handling system (controlling the valves for the introduction of electrolytes and samples) and a conductivity detector, all of which are operated using a program written in LabVIEW v6.1 (National Instruments, Austin, TX, USA). Either a four-way 1.5-kV constant voltage PSU with a fluid handling system and conductivity detection, documented in Ref. [27], or a six-way PSU was used. The six-way PSU can operate either in a constant voltage or constant current mode, and can supply up to 4 kV and may be used up to 150 μ A (in constant current mode). The six-way PSU is embedded in a complete microdevice control system that incorporates a fluid handling system and enables conductivity detection. The control system uses four National Instruments cards. A PCI-6503 controls the valves through a

Table 1
Summary of electrode designs

	Electrode design 1	Electrode design 2	Electrode design 3
Electrode material	8% carbon black-filled polystyrene	40% carbon fibre-filled nylon 6/6	40% carbon fibre-filled polystyrene
Chip material	Polystyrene	Zeonor	Polystyrene
Channel width (μm)	300	100	200
Channel depth (μm)	50	400	200
Separation channel length (mm) ^a	19.9	Straight channel: 19.2 Meander channel: 74.2	(a) 1D chip: 44 (b) 2D chip: 54.4 1st dimension: 29 2nd dimension 25.4
Electrode parameter (μm) ^b	Width: 200 Length: 100	Width: 160 Height: 200	Width: 160 Height: 200

^a Measured from the centre of the injector to the middle of the detection electrodes.

^b Design one has electrodes flush with the bottom of the channel, while designs two and three have electrodes flush with the channel sides, as depicted in Fig. 4.

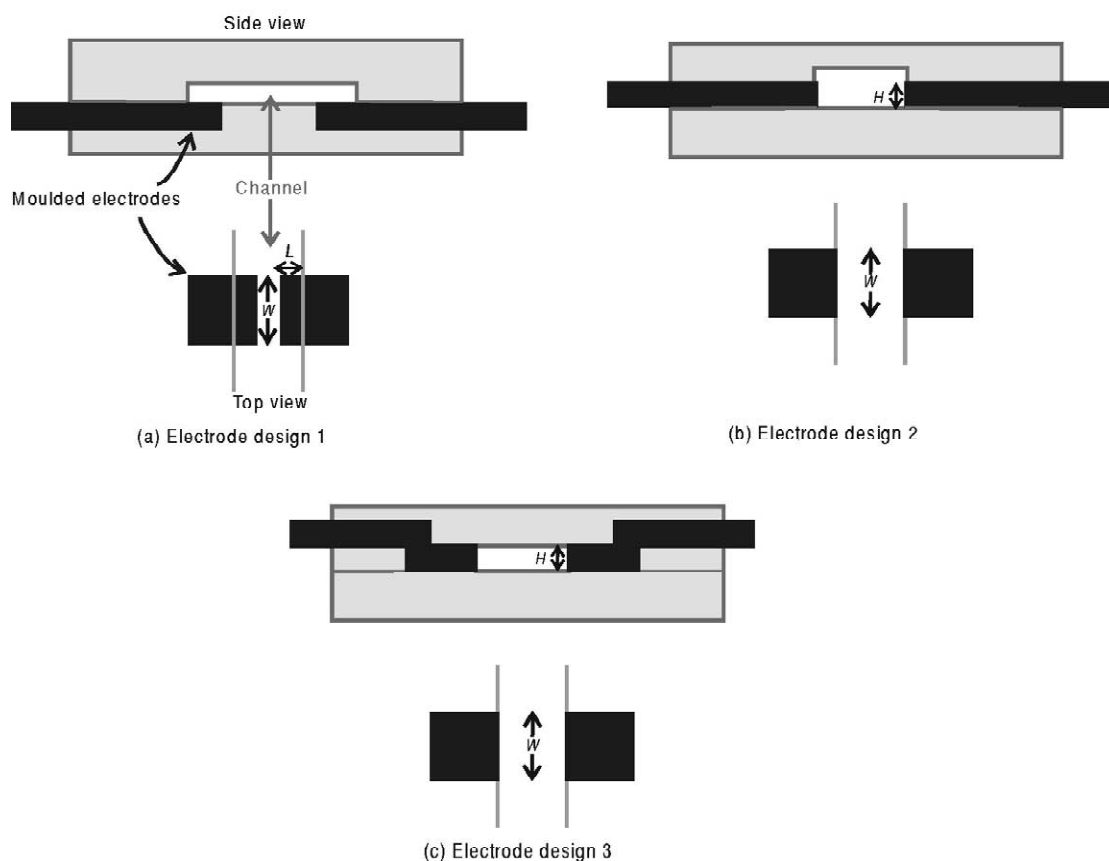


Fig. 4. Depicts side and top views of the three fabricated electrode designs. Values of electrode widths (W), electrode heights (H) and electrode length (L) are given in Table 1.

DI0-24 MX relay box (Goldchip, Wimbourne, UK). A PCI-6713E provides the PSU voltage control and valve timing clock. A PCI-6023E enables current monitoring of the PSU for constant current mode operation. A PCI-6602 drives the conductivity detector. The six-way PSU consists of six HV modules (4A12-P4, Ultravolt, Ronkonkoma, NY, USA), and two relays (HE12-1A83, Meder, Berlin, Germany) so that each of the six outputs of the PSU can be connected to ground, module output, or left floating. There is also a bleed resistor (20 M Ω) on the output of each module, so that when the relays connect the module output to the respective PSU output, the PSU output may either sink or source current. The PSU modules each have a current monitor output; these were calibrated using precision resistors. The bleed resistor values were also measured. This allows the output current of each module to be calculated in the control program and hence a feedback loop can be established to provide constant current.

Conductivity detection was performed mainly using a capacitatively coupled (to enable isolation from the HV) conductivity detector, based on an astable oscillator, reported in 2000 [28]. A capacitatively coupled resistive divider was also investigated for performing conductivity detection with the injection moulded electrodes. This detector oscillates at 1 kHz and gathers instantaneous voltage readings 3 μ s after each edge of the generated square wave. The difference between successive readings is taken to give a 1 kHz data stream. Groups of 50 values are then averaged to produce a 20 Hz output trace. This detector was controlled with a PCI-6024E data acquisition card programmed using LabVIEW via the NI-DAQ device driver system [29].

The fluid handling system is gravity fed and comprises of a component board fitted with valves and solution reservoirs (formed from 20-ml syringe barrels) housed within a HV safety enclosure. Solenoid valves (Series LFVA1210120 H, Lee Products, Gerrards Cross, UK) and narrow bore Teflon tubing (0.032 in. I.D., Lee Products; 1 in.=2.54 cm) were used to effect the ingress and outgress of the electrolytes and samples to the microdevice. A pressure of 2157 N m⁻² was used throughout this study. Fig. 5 depicts a typical set-up for performing a miniaturised ITP separation. A typical analysis program would be to open the valves to the LE reservoir

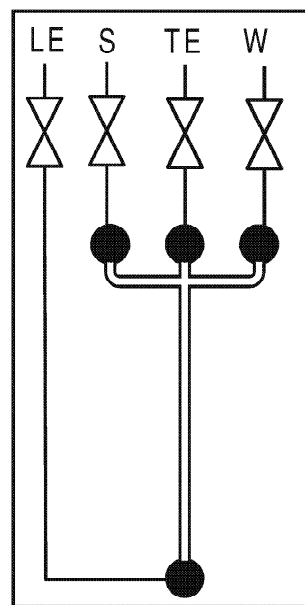


Fig. 5. Typical connection set-up for the valve-controlled electrolyte and sample introduction system for performing ITP separations on a microdevice where LE is the leading electrolyte, S is the sample, TE the terminating electrolyte and W is the waste.

and the waste reservoir and flush LE through the system. The valve to the LE reservoir would then be closed and the one to the TE reservoir opened so that TE could be flushed through to waste. The TE valve was then shut and the sample reservoir opened and sample flowed through the injection cross to waste. All valves were then closed before the HV separation stage commenced.

2.4. LabVIEW data analysis

Zone boundaries are identified using a data analysis program which takes the derivative of the filtered data and then determines the maxima using a standard algorithm which attempts to fit quadratic curves. An elliptic filter was chosen as it has the same phase response for all frequencies thereby minimising any effect on zone lengths. Four parameters control the resulting output: filter cut-off frequency, filter order, minimum peak height and peak width.

3. Results and discussion

3.1. Evaluation of conductivity electrodes and device fabrication

Table 2 presents the results of the investigation into the characterisation of the detection electrodes with respect to their suitability for performing conductivity detection. To carry out this study the microdevices were connected to the capacitively coupled detector circuit and a standard conductivity cell calibrating solution (0.1 M KCl) was injected into the channel and the frequency response of the detector monitored. The cell constant was also calculated from Eq. (1):

$$K_{\text{cell}} = \kappa R \quad (1)$$

where K_{cell} is the cell constant, κ is the standard conductivity of a KCl solution of known concentration (1.116 S m⁻¹ at 18 °C for 0.1 M KCl) [30] and R the observed cell resistance required to produce the observed frequency response. For the first design of microdevices using 8% carbon black-filled polystyrene electrodes, six devices were studied and responses to 0.1 M KCl ranging from 0 to 1.8 kHz were obtained. This proved to be too insensitive for performing conductivity detection. The poor performance of the electrodes was due to the low conductivity of the carbon-black-filled polystyrene. Hence, a less resistive grade of conducting polymer was sought, and carbon fibre grades were considered. In addition a bonding method less prone to causing channel blockage than gluing was investigated and lamination methods were used for all subsequent devices. The second set of electrodes made from 40% carbon fibre-filled nylon 6/6 was

tested in the same manner. The obtained frequency responses were better with an average frequency response of 97±22 kHz (standard deviation) being achieved for three devices. Hence, conductivity detection could be performed on these devices. Although these devices gave an enhanced conductivity response compared to design one, the dissimilarity in the nature of the nylon electrodes and the Zeonor chip led to fabrication problems, with devices frequently failing due to poor bonding of the nylon electrodes into the Zeonor. This poor adhesion could often lead to undesirable leakage of solutions between the two plastics. In order to circumvent this problem a third design of electrode was explored. This third design of electrode was three-dimensionally structured so that electrode contact was made through the top of the device. This structuring of the electrodes meant that more injection moulded plastic surrounded the electrodes leading to less solution leakage problems. In addition the raising of the electrodes to the top of the chip enabled another separation channel (2D separation chip) to be incorporated in the design by passing the extra channel underneath the connectors for the detection electrodes (see Fig. 3b). Using a 40% carbon fibre-filled polystyrene electrode material in a polystyrene chip also gave a desired improvement in the frequency response, and solely using polystyrene polymers meant that the chip materials were compatible, which led to enhanced bonding and better performance for conductivity detection. Typical frequency response values were 134±9 kHz (standard deviation). Calculated cell constants for the two successful electrode designs are presented in Table 2. Fig. 6 shows a microdevice incorporating injection moulded carbon fibre electrodes (electrode design three); good align-

Table 2
Comparison of electrode designs for conductivity detection

	40% Carbon fibre-filled nylon 6/6 electrodes (electrode design 2)	40% Carbon fibre-filled polystyrene electrodes (electrode design 3)
Electrode parameters (µm)	Width:160 Height: 200	Width:160 Height: 200
Frequency response (kHz)	97±22 (<i>n</i> = 3)	134±9 (<i>n</i> = 5)
Cell constant (cm ⁻¹)	104±20	95±2

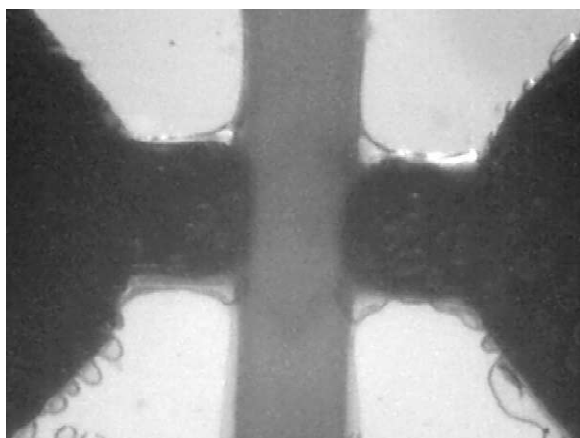


Fig. 6. A pair of carbon fibre-filled polystyrene electrodes of 200 μm width and 200 μm height. The separation channel is 200 μm wide by 200 μm deep. The channel is filled with amaranth dye (0.01 M).

ment of the electrodes with the channel walls was observed. Testing with a dye (0.01 M amaranth) indicated that the device was fully bonded.

3.2. Evaluation of high voltage performance

To ensure that the injection moulded devices were capable of performing under HV conditions, the electrical characteristics were investigated. This was carried out by measuring the generated capillary current versus the applied voltage (I – V). The I – V characteristics were measured using the six-way computer-controlled PSU to increase the voltage every 20 s and record the resulting current at 0.05-s time intervals. Data points in Fig. 7 represent the average current readings ± 1 standard deviation. The response of both the LE (0.02 M NaOH, 0.015 M HIBA, pH 4.95) and TE (0.01 M carnitine), both with added HEC 0.05% (w/v), were examined. From the results shown in Fig. 7, it can be seen that a linear response was attained for the LE up to a potential of 500 V. The response from the lower conductivity TE was linear up to 800 V. Previous investigations of the I – V response of miniaturised devices constructed solely from silicone elastomer

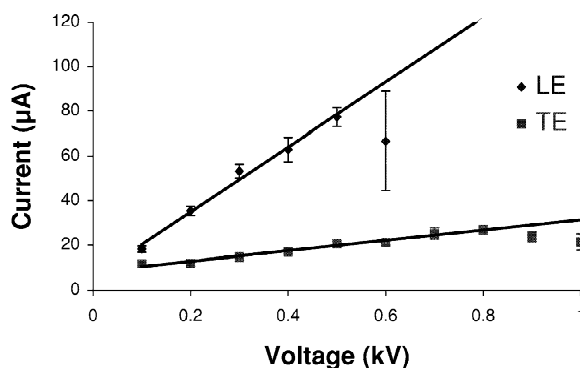


Fig. 7. Current–voltage plot for the injection moulded devices. The LE was 0.02 M NaOH, with 0.015 M HIBA adjusted to pH 4.95 and the TE was 0.01 M carnitine, both had added HEC 0.05% (w/v).

(PDMS) [12] show a deviation from linearity from a point that corresponds to the microdevices being no longer able to dissipate efficiently the Joule heat from the microchannels. However, in this study the response to increasing the applied voltage was found not to be a gradual decline in dissipation efficiency but a sudden decrease. This was due to the failure of the adhesive laminate used in device bonding. The maximum amount of power that the injection moulded devices can dissipate can be calculated from the end point of the linear response. It was found that the microdevices could dissipate 1.4 W m^{-1} with LE and 0.8 W m^{-1} when filled with TE. This is higher than the 1 W m^{-1} reported for silicone elastomer devices [31]. Though less than the 2.8 W m^{-1} power dissipation experienced with glass devices [32]. This is to be expected due to the lower thermal conductivities of polymers, typically less than 0.3 $\text{W m}^{-1} \text{K}^{-1}$ [33], compared to glass, which has values around 1 $\text{W m}^{-1} \text{K}^{-1}$ [30]. The resistance of the channel when filled with LE was determined to be 6.9 and 43.6 $\text{M}\Omega$ when filled with TE. To avoid excess heating in the separation channel, and thus possibly causing detrimental effects on the separation performance, the maximum amount of power supplied for most separations was less than 1 W m^{-1} and the current supplied for constant current separations was set at 30 μA or under.

3.3. Evaluation of the fabricated microdevices for ITP separations

The injection moulded devices were used to successfully separate several model mixtures. Figs. 8–10 show the resulting isotachopherograms from separations of anionic dyes, inorganic anions and metal cations, respectively. The anion separations were performed using the four-way PSU and capacitatively coupled astable oscillator conductivity detector. The microdevice employed was the conducting nylon 6/6 electrode device (electrode design two) with a Zeonor channel. Separations of the anions were quite fast with analysis times of 2 min for a separation of three anionic dyes; amaranth, bromophenol blue and methyl orange (see Fig. 8), and under 3 min for a separation of nitrite and fluoride (see Fig. 9). Step heights were found to be reproducible, analysis of ITP separations of amaranth gave a relative step height (RSH) of 0.512 ± 0.01 ($n = 15$) (where RSH is the height difference between the sample and the leading electrolyte response divided by the height difference between the terminating electrolyte and the leading electrolyte). Six amaranth samples with concentrations ranging from

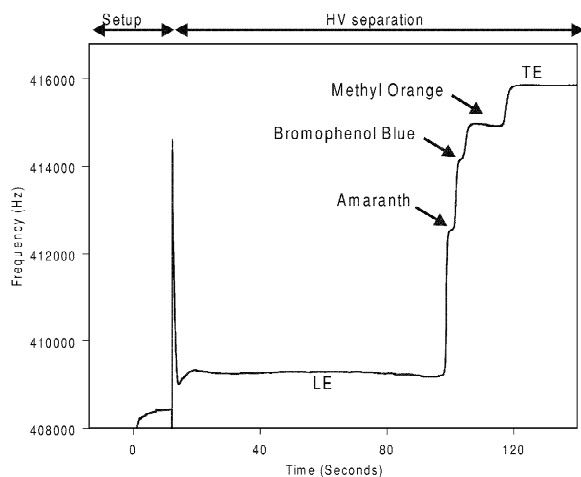


Fig. 8. Isotachopherogram of a separation of three anionic dyes. LE, 0.01 M HCl, pH 6 (histidine), 0.1% (w/v) HEC; TE, 0.01 M MES, pH 6 (histidine). Sample, amaranth, bromophenol blue both 5×10^{-4} M, methyl orange 1×10^{-3} M. Injection procedure, LE flush 5 s, TE flush 5 s, sample flush 5 s. Separation voltage, 600 V. Microdevice details, as given for electrode design two (straight channel) in Table 1.

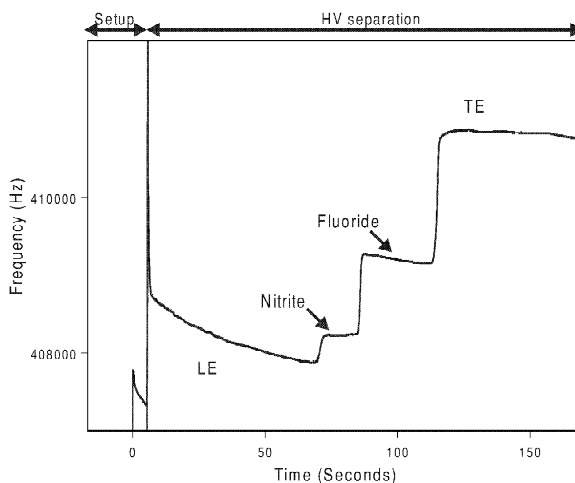


Fig. 9. Isotachopherogram of a separation of two inorganic anions. LE, 0.01 M HCl, pH 3.6 (glycylglycine), 0.1% (w/v) HEC; TE, 0.01 M benzoic acid. Sample, fluoride 10 ppm and nitrite 50 ppm. Injection procedure, LE flush 3 s, TE flush 3 s, sample flush 2 s. Separation voltage was 600 V. Microdevice details, as given for electrode design two (straight channel) in Table 1.

1×10^{-5} M to 5×10^{-4} M were analysed and zone lengths determined, a linear response was obtained ($y = 36620x + 1.305$, $R^2 = 0.98$, $n = 3$) over the concentration range. The analysis used the following

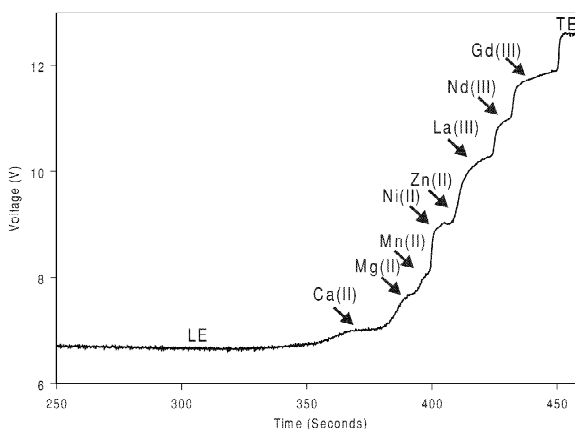


Fig. 10. Isotachopherogram of a separation of eight metal cations. LE, 0.02 M NaOH, with HIBA (0.015 M), pH 4.95, 0.05% (w/v) HEC. TE, 0.01 M carnitine hydrochloride. Sample, all 8×10^{-4} M except Mg(II) which was 1×10^{-3} M. Injection procedure, TE flush 5 s, LE flush 20 s, sample flush 2 s. Separation current was 20 μ A. Microdevice details, as given for electrode design three (1D column device) in Table 1.

set-up. LE was flushed through the chip to waste for 5 s, then TE for 5 s and then sample was flowed through the cross injector for 3 s. The separation voltage was 600 V. Step heights and zone lengths were determined using LabVIEW data analysis. The separation of metal cations was initially investigated using the six-way PSU and the capacitatively coupled astable oscillator conductivity detector. However, the response range of the detector was found to be deficient for this electrolyte system, so another type of detector was constructed to overcome the lack of sensitivity. Use of the capacitatively coupled resistive divider conductivity detector improved the response and enabled conductivity detection of metal cation separations to be achieved on the injection moulded devices. Fig. 10 shows an isotachopherogram of an eight component metal cation mixture. Analysis was achieved in 7.5 min on a 44-mm-long channel (1D chip version of the third electrode design). Table 3 presents the RSHs determined for the cations investigated. Step identification was determined by performing ITP separations of individual metal components. ITP studies of similar mixtures of metal ions separated on a conventional capillary isotachopheresis instrument (ItaChrom EA101, J&M Analytische Messung und Regeltechnik, Aalen, Germany) found that up to six metals can be separated on the first column (90 mm×0.8 mm I.D.) within 14 min [34]. Speeding up the analysis time means that isotachopheresis becomes more amenable for use as an on-line analysis technique.

Polarization of the detection electrodes due to the applied separation current could cause evolution of hydrogen and oxygen in addition to causing other redox reactions. These electrochemical reactions

would have a detrimental effect on the ITP analyses, as reported by Everaerts and Verheggen [35]. The use of a high frequency AC detection circuit reduces the likelihood of these reactions occurring. Microscope observations (with a resolution of 10 μm) of the detection electrodes carried out while ramping the applied potential from 50 V to 1.5 kV across the LE (for the metal cation system)-filled separation channel showed no bubble formation, a typical metal separation started at 300 V and ended at 1.1 kV. No signs of bubble formation at the electrodes were observed during microscope-monitored ITP separations. If a layer of gas bubbles had accumulated on the electrode surface during separations an increase in the noise of the conductivity detector trace and distortion of the measured zone boundaries would have been apparent. In addition, degradation or coating of the electrodes would result in shifts from run-to-run in the baseline of the detector. Analysis of the amaranth separations gives a frequency value of 409.44 ± 0.31 kHz ($n=18$) for the LE and 415.95 ± 0.15 kHz ($n=18$) for the TE indicating that the response of the detector was stable and no detrimental electrode phenomena were observed in the electrolyte and sample systems studied. The carbon fibre-filled polystyrene electrode material has been evaluated for its electrochemical (voltammetric) behaviour and shows similar properties to glassy carbon over the potential range -250 to $+400$ mV (vs. Ag/AgCl), in 0.1 M HNO₃. The miniaturised injection moulded devices were found to be suitable for performing ITP separations and although these mass produced, low cost injection moulded devices are designed for disposable applications they are actually quite long lasting. For example one microdevice was used for over 230 separations.

Table 3
Analysis of RSHs of ITP separations of an eight-component metal mixture ($n=4$)

Metal	Relative step height (RSH)
Ca(II)	0.063 ± 0.006
Mg(II)	0.115 ± 0.051
Mn(II)	0.210 ± 0.026
Ni(II)	0.403 ± 0.023
Zn(II)	0.413 ± 0.023
La(III)	0.620 ± 0.018
Nd(III)	0.749 ± 0.018
Gd(III)	0.878 ± 0.014

4. Conclusion

Devices containing drive and detection electrodes have been fabricated from three different grades of conducting polymer and two different microdevice materials. The produced devices have been evaluated for performing ITP separations. Two of the electrode designs were found to be suitable for carrying out integrated conductivity detection. Analysis of several model test mixtures was carried out. Hence, the

feasibility of constructing microdevices solely from polymers using mass fabrication techniques has been demonstrated.

Acknowledgements

The authors gratefully acknowledge Dr. Anastasios Economou (Department of Chemistry, Aristotle University of Thessaloniki, Greece) for the voltammetric studies. Financial support was provided by the Engineering and Physical Research Council (EPSRC, UK), the European Union and the Medical Research Council (MRC, UK) via the North West Science Review.

References

- [1] H. Becker, L.E. Locascio, *Talanta* 56 (2002) 267.
- [2] H. Becker, C. Gartner, *Electrophoresis* 21 (2000) 12.
- [3] P. Boček, M. Deml, J. Janák, *J. Chromatogr.* 106 (1975) 283.
- [4] P. Gebauer, M. Deml, P. Boček, J. Janák, *J. Chromatogr.* 267 (1983) 455.
- [5] L.W. Pickering, S.J. Baldock, P.R. Fielden, N.J. Goddard, R.D. Snook, B.J. Treves Brown, in: D.J. Harrison, A. van den Berg (Eds.), *Proceedings of the μ TAS'98 Workshop*, Banff, Canada, 13–16 October, 1998, Kluwer, Dordrecht, 1998, p. 101.
- [6] S.J. Baldock, N.J. Goddard, P.F. Fielden, in: *Proceedings of MICRO.tec 2000*, VDE Verlag, Hannover, Germany, 2000, p. 615.
- [7] S.J. Baldock, N. Bektaş, P.R. Fielden, N.J. Goddard, L.W. Pickering, J.E. Prest, R.D. Snook, B.J. Treves Brown, D.I. Vaireanu, in: D.J. Harrison, A. van den Berg (Eds.), *Proceedings of the μ TAS'98 Workshop*, Banff, Canada, 13–16 October, 1998, Kluwer, Dordrecht, 1998, p. 359.
- [8] P.R. Fielden, S.J. Baldock, N.J. Goddard, L.W. Pickering, J.E. Prest, R.D. Snook, B.J. Treves Brown, D.I. Vaireanu, in: D.J. Harrison, A. van den Berg (Eds.), *Proceedings of the μ TAS'98 Workshop*, Banff, Canada, 13–16 October, 1998, Kluwer, Dordrecht, 1998, p. 323.
- [9] S.J. Baldock, P.R. Fielden, N.J. Goddard, J.E. Prest, B.J. Treves Brown, in: *Proceedings of the 24th International Symposium on Capillary Chromatography and Electrophoresis*, 20–24th May, 2001, Las Vegas, NV, 2001, <http://www.meetingabstracts.com>.
- [10] P.R. Fielden, S.J. Baldock, N.J. Goddard, J.E. Prest, B.J. Treves Brown, in: *Proceedings of the 24th International Symposium on Capillary Chromatography and Electrophoresis*, 20–24th May, 2001, Las Vegas, NV, 2001, <http://www.meetingabstracts.com>.
- [11] J.E. Prest, S.J. Baldock, N. Bektaş, P.R. Fielden, B.J. Treves Brown, *J. Chromatogr. A* 836 (1999) 59.
- [12] J.E. Prest, S.J. Baldock, B.J. Treves Brown, P.R. Fielden, *Analyst* 126 (2001) 433.
- [13] P.R. Fielden, S.J. Baldock, N.J. Goddard, J.E. Prest, B.J. Treves Brown, in: *Proceedings of MICRO.tec 2000*, 25–27th September, 2000, Hannover, Germany, VDE Verlag, Berlin, 2000, p. 25.
- [14] P.R. Fielden, S.J. Baldock, N.J. Goddard, L. Morrison, J.E. Prest, B.J. Treves Brown, M. Zraggen, in: D.J. Bornhop, D.A. Dunn, R.P. Mariella, C.J. Murphy, D.V. Nicolau, M. Palmer, R. Raghavachari (Eds.), *Proceedings of SPIE Volume 4626: Biomedical Nanotechnology Architectures and Applications*, SPIE, Bellingham, WA, 2002, p. 429.
- [15] B. Grass, A. Neyer, M. Jöhnck, D. Siepe, F. Eisenbeiss, G. Weber, R. Hergenröder, *Sensors Actuators B-Chem* 72 (2001) 249.
- [16] M. Masár, D. Kaniansky, R. Bodor, M. Jöhnck, B. Stanislawski, *J. Chromatogr. A* 916 (2001) 167.
- [17] D. Kaniansky, M. Masár, J. Bieličková, F. Iványi, F. Eisenbeiss, B. Stanislawski, B. Grass, A. Neyer, M. Jöhnck, *Anal. Chem.* 72 (2000) 3596.
- [18] E. Ölvecká, M. Masár, D. Kaniansky, M. Jöhnck, B. Stanislawski, *Electrophoresis* 22 (2001) 3347.
- [19] M. Masár, M. Zúborová, J. Bieličková, D. Kaniansky, M. Jöhnck, B. Stanislawski, *J. Chromatogr. A* 916 (2001) 101.
- [20] B. Grass, D. Siepe, A. Neyer, R. Hergenröder, *Fresenius J. Anal. Chem.* 371 (2001) 228.
- [21] R. Bodor, V. Madajová, D. Kaniansky, M. Masár, M. Jöhnck, B. Stanislawski, *J. Chromatogr. A* 916 (2001) 155.
- [22] R. Bodor, M. Zúborová, E. Ölvecká, V. Madajová, M. Masár, D. Kaniansky, B. Stanislawski, *J. Sep. Sci.* 24 (2001) 802.
- [23] B. Grass, R. Hergenröder, A. Neyer, D. Siepe, in: *Proceedings of the 24th International Symposium on Capillary Chromatography and Electrophoresis*, 20–24th May 2001, Las Vegas, NV, 2001, <http://www.meetingabstracts.com>.
- [24] M. Zúborová, M. Masár, D. Kaniansky, M. Jöhnck, B. Stanislawski, *Electrophoresis* 23 (2002) 774.
- [25] V. Krivtun, B. Grass, R. Hergenröder, M. Bolshov, K. Niemax, A. Zybin, *Appl. Spectrosc.* 55 (2001) 1251.
- [26] P.A. Walker, M.D. Morris, M.A. Burns, B.N. Johnson, *Anal. Chem.* 70 (1998) 3766.
- [27] J.E. Prest, S.J. Baldock, P.F. Fielden, N.J. Goddard, B.J. Treves Brown, *Analyst* 127 (2002) 1413.
- [28] D.-I. Vaireanu, P.R. Fielden, B.J. Treves Brown, *Measur. Sci. Technol.* 11 (2000) 244.
- [29] B.J. Treves Brown, P.R. Fielden, in preparation.
- [30] D.R. Lide, *CRC Handbook of Chemistry and Physics*, Chemical Rubber, Boca Raton, FL, 1993.
- [31] C.S. Effenhauser, G.J.M. Bruin, A. Paulus, M. Ehrat, *Anal. Chem.* 69 (1997) 3451.
- [32] Z.H. Fan, D.J. Harrison, *Anal. Chem.* 66 (1994) 177.
- [33] 15th ed., *Lange's Handbook of Chemistry*, McGraw-Hill, London, 1999.
- [34] J.E. Prest, Ph.D. Thesis, UMIST, Manchester, 2000.
- [35] F.M. Everaerts, Th.P.E.M. Verheggen, *J. Chromatogr.* 73 (1972) 193.